Ingo Förtsch
Hartmut Fritzsche
Institute of Molecular Biology
Friedrich-Schiller University
Jena
Winzerlaer Strasse 10
D-07745 Jena, Germany

Eckhard Birch-Hirschfeld
Institute of Molecular
Biotechnology
Beutenbergstrasse 11
D-07745 Jena, Germany

Elisabeth Evertsz
Reinhard Klement
Thomas M. Jovin
Department of Molecular
Biology
Max-Planck Institute for
Biophysical Chemistry
Postfach 2841
D-37018 Göttingen, Germany

Christoph Zimmer
Institute of Molecular Biology
Friedrich-Schiller University
Jena
Winzerlaer Strasse 10
D-07745 Jena, Germany

Parallel-Stranded Duplex DNA Containing dA · dU Base Pairs

DNA oligonucleotides with dA and dU residues can form duplexes with trans *d(A · U) base pairing and the sugar–phosphate backbone in a parallel-stranded orientation, as previously established for oligonucleotides with d(A · T) base pairs. The properties of such parallel-stranded DNA (ps-DNA) 25-mer duplexes have been characterized by absorption (uv), CD, ir, and fluorescence spectroscopy, as well as by nuclease sensitivity. Comparisons were made with duplex molecules containing (a) dT in both strands, (b) dU in one strand and dT in the second, and (c) the same base combinations in reference antiparallel-stranded (aps) structures. Thermodynamic analysis revealed that total replacement of deoxythymine by deoxyuridine was accompanied by destabilization of the ps-helix (reduction in* T_m *by −13°C in 2 m*M *$MgCl_2$, 10 m*M *Na-cacodylate). The U-containing ps-helix (U1 · U2) also melted 14°C lower than the corresponding aps-helix under the same ionic conditions; this difference was very close to that*

Received March 6, 1995; accepted June 7, 1995.
Biopolymers, Vol. 38, 209–220 (1996)
© 1996 John Wiley & Sons, Inc.
CCC 0006-3525/96/020209-12

observed between ps and aps duplexes with d(A·T) base pairs. Force field minimized structures of the various ps and aps duplexes with either d(A·T) or d(A·U) base pairs ps/aps and dT/dU combinations are presented. The energy-minimized helical parameters did not differ significantly between the DNAs containing dT and dU. © *1996 John Wiley & Sons, Inc.*

INTRODUCTION

The structure and properties of parallel-stranded double-helical DNA (ps-DNA) incorporating d(A·T) base pairs have been investigated in detail[1-9] and provide confirmation for the model building and theoretical predictions of Pattabiraman[10] and Kuryavyi.[11] In ps-DNA, both strands have the same 5′-3′ polarity. The secondary structure is stabilized by reverse Watson–Crick base pairing characterized by a *trans* orientation of the glycosidic bonds and H bonding via the O2 instead of the O4 keto group of the pyrimidine.[6-9] The latter features have been confirmed by Raman[8] and ir[9] spectroscopy of ps- and aps-DNA. Using spectroscopic, thermodynamic, and biochemical methods, it has been shown that ps-DNA differs considerably from antiparallel-stranded DNA (aps-DNA). The *trans* base pairing in ps-DNA leads to two equivalent grooves,[7,11,12] in contrast to the classical major/minor grooves of B-DNA, i.e., aps-DNA. The two-stranded DNA duplexes of the ps form constructed to date have consisted of d(A·T) and of d(G·C) base pairs[2,3,5] or alternating d(G-A) sequences with d(G·G) and d(A·A) base pairs.[12] Isolated d(G·C) base pairs in the 25-nt d(A·U) sequences cause a destabilization of the helix, as evidenced by lower transition enthalpies and T_m values,[5,13] although up to 40% substitution in other sequence contexts maintains the ps configuration.[14] Evidence for a B-to-A-like transition in such molecules has been reported.[15]

The static and dynamic polymorphism of ps duplexes is extensive, both by computational[16] (V. Kuryavyi and T. M. Jovin, in preparation) and experimental analysis. For example, ps duplexes form readily from synthetic oligonucleotides comprised of adjoining purine–purine and purine–pyrimidine base-paired segments.[17] It was demonstrated that a block of alternating $d(GA)_n$ yields a ps homoduplex of d(G·G) and d(A·A) base pairs next to a block of a ps segment of *trans* d(A·T) base pairs. Pyrimidine–pyrimidine pairing, notably in the form of half-protonated $d(C^+ \cdot C)$ base pairs, are present in ps duplexes examined under acidic conditions by nmr.[18] In higher order (n-stranded) structures, at least $n(n-1)/2 - 1$ relationships between any two strands have to be parallel (though not necessarily hydrogen bonded) from fundamental geometric considerations. For example, a ps-helix with Hoogsten base pairs has been claimed to be a component of a triple helix.[19] The nmr and x-ray crystallographic analyses have also revealed the existence of four-stranded structures consisting of intercalated ps duplexes formed from oligopyrimidine sequences.[20,21] Unfortunately, such high-resolution three-dimensional data for ps duplexes such as those reported in the present study are not yet available.

In view of the unique helical properties of ps-DNA, in which the C5 methyl group of T can be positioned in either or both grooves depending on the sequence, it was of interest to analyze molecules with d(A·T) base pairs substituted by d(A·U) base pairs. This report deals with such an investigation in which ps and corresponding aps duplexes were compared using a variety of techniques. Parallel-stranded helices containing dU can form in 2 mM $MgCl_2$ and 10 mM Na^+, albeit with lower stability than reference molecules incorporating dT.

MATERIALS AND METHODS

Oligonucleotide Synthesis

The syntheses of oligonucleotides U1, U2, and U3 (Figure 1) were carried out using Applied Biosystems Model 380B and 394 DNA/RNA synthesizers. 5′-O dimethoxytrityldeoxy-nucleoside-3-O-(2-cyano)-N,N-

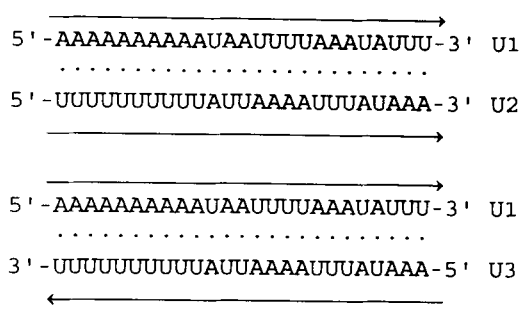

FIGURE 1 Sequences of oligonucleotide duplexes. Duplexes are denoted by U1·U2 and U1·U3, respectively. The D-series duplexes are the thymine containing oligomers studied previously.[28]

diisopropylaminophosphanes were from MWG Biotech and deoxyuridine-CE-phosphoramidite from Beckmann and Cruachem. The standard solutions for activation, oxidation, and detritylation were also from these companies. Small amounts [up to 20 optical density (OD) units] of oligonucleotides were purified by high performance liquid chromatography (HPLC) using a BioRad Model 2700; larger quantities were purified by fast protein liquid chromatography (Pharmacia) using a Resource Q (6 mL) column.

Oligonucleotides for pyrene labeling reactions were synthesized with a primary amino group linked to the 5'-end using the Aminolink-2 reagent from Applied Biosystems. Small amounts (up to 20 OD units) of the deblocked oligonucleotides were purified by HPLC using a Mono Q HR 5/5 anion exchanger column (Pharmacia; gradient buffer A: 10 m*M* NaOH, 0.1 NaCl pH 11; buffer B: 10 m*M* NaOH, 1 *M* NaCl pH 11, 0–100% in 30 min). After desalting on DEAE Sephadex and drying, the modified oligonucleotides (25–30 OD units) were dissolved in 0.5 mL of 0.3 *M* Na-bicarbonate and 0.8 mL dioxane. To this solution 0.25 mL of a freshly prepared 20–30 mg/mL stock of succinimidyl-1-pyrenebutyrate (Molecular Probes) in dry dimethyl formamide were added and the reaction was allowed to proceed as in Ref. 12. After removal of the free dye by Sephadex G25 the pyrene labeled oligonucleotides were separated from unreacted material by reversed-phase HPLC on a Eurosil-Bioselect 300-C18, 5 μm column (Knauer). An acetonitrile gradient in 0.1 *M* triethylammonium acetate (TEAA), pH 7, was used for separation. Elution was monitored by uv spectroscopy.[12] The unreacted oligonucleotides appeared in the first and the labeled material in the second peak (0.1 *M* TEAA, gradient 0–50% acetonitrile in 20 min followed by 50–100% acetonitrile in 5 min, flow rate 1.4 mL/min). The collected fraction from the HPLC run was dried and precipitated by addition of ethanol to remove any traces of TEAA buffer. The purity of the pyrene labeled oligonucleotides was controlled by uv spectroscopy as described earlier.[12]

The purity of the isolated oligonucleotides and the formation of duplex structures were established by gel electrophoresis under native conditions (14% acrylamide, 5% cross-linking, 90 m*M* Tris-borate 2 m*M* $MgCl_2$, pH 8.0 at 4°C) and visualized by Stains All (Serva): 50 mg/L in 2.5% formamide, 25% isopropanol, and 30 m*M* Tris-borate, pH 8.8.

Enzymatic Reactions

Nuclease studies were performed as follows: DNase I (Calbiochem): 40 m*M* Tris-HCl, pH 7.5, 3.3 m*M* $MgCl_2$, 0.2 m*M* $CaCl_2$; *Escherichia coli* exonuclease III (Boehringer, Mannheim): 50 m*M* Tris-HCl, pH 8.0, 5 m*M* $MgCl_2$, 10 m*M* 2-mercaptoethanol. The products of the enzymatic reaction were analyzed by polyacrylamide gel electrophoresis under denaturing conditions[4] (20% polyacrylamide, 5% cross-linking, 8 *M* urea, 90 m*M* Tris-borate, 2 m*M* EDTA, pH 8.0).

Spectroscopy

The uv absorption measurements were performed on a Cary 1E spectrophotometer (Varian) equipped with a thermostated cell holder. The molar extinction coefficients of the oligonucleotides at 260 nm and 70°C, determined by phosphate analysis, were as follows: U1, $8600 M^{-1}$ cm^{-1}; U2 and U3, $8800 M^{-1}$ cm^{-1}. For the d(A·T) containing duplexes the corresponding values used for D1, D2, and D3 were $8600 M^{-1}$ cm^{-1} at 264 nm at 70°C.[2,5,6] The thermodynamic parameters of the two-state helix-coil thermal transitions[3,17] were determined by two methods: (a) A^{266} vs. T records (Cary) were acquired with a continuous temperature increment of 0.5°/min; the curves (ascending limbs) were smoothed and $\partial A^{266}/\partial T$ values computed with Savitzky-Golay filters. (b) Temperature-resolved spectra were measured and analyzed according to Refs. 3 and 17. The T_m values were corrected to a reference total strand concentration of 1 μM.[17]

Fluorescence measurements were made with a SLM Aminco 48000 spectrofluorimeter at 4°C. For drug binding studies DNA was added with a 0.5–10 μL microsyringe.

CD spectra were recorded on a Jasco Model 720 CD dichrograph using a 1 cm path-length cell at 4°C. All measurements were made in standard buffer solution (2 m*M* $MgCl_2$, 10 m*M* Na-cacodylate, pH 7.0) unless stated otherwise.

Infrared spectra were recorded at a resolution of 1 cm^{-1} using a Mattson Galaxy 4020 Fourier transform ir spectrophotometer. The solution spectra in H_2O and D_2O were taken as described previously.[9] The final solutions contained 175 m*M* DNA, 30 m*M* $MgCl_2$, and 150 m*M* NaCl. The spectra were processed using GRAMS/386 (Galactic Industries). Smoothing by the Savitzky-Golay algorithms with 5, 7, and 11 points was applied, and the baseline was corrected for the solvent. The precision of the frequency was 1 cm^{-1}.

Model Structure Calculations

Force field calculations were with (AMBER) v. 4.0.[22,23] The start conformations for the d(A·U) structures were generated as d(A·T) structures with NAMOT v. 1.2S.[24] To construct the ps conformers, two aps structures (D1·D3 and D2·D4) were first created. The strands in each duplex were separated, and the D2 strand was rotated and joined with D1. The edit module of the AMBER package replaced the thymine by uracil bases where desired.

To minimize the dA·dU structures, a DURA entry had to be added to the AMBER data base.[18] The structures were minimized with the AMBER v. 4.0 force field parameters, a distance-dependent dielectric constant with the initial value $\varepsilon = 2$, and a nonbonded cutoff of 25 Å. No constraints were imposed on the structures during minimization. The latter was terminated when the rms

of the gradient norm dropped below 0.05. The AMBER calculations were carried out on an SGI Indy R4400SC RISC workstation and took ~ 25 central processing unit (CPU) min for the aps and ~ 27 CPU min for the ps structures.

The helical parameters of the DNA conformers were calculated with GEOM.[23,24] CPK models were generated with SCHAKAL92 (E. Keller, University of Freiburg, Germany).

RESULTS AND DISCUSSION

Duplex Formation from UV Absorption Spectroscopy

The 25-nt sequences (U1, U2, and U3 in Figure 1) were used to generate the complete set of d(A·U) duplexes in analogy to the d(A·T) containing ps and aps duplexes shown previously for D1, D2, and D3.[2,6] The formation of duplexes at 4°C was monitored by polyacrylamide gel electrophoresis as in Ref. 2. There were no differences in the migration of dA·dU and d(A·T) containing ps duplexes, nor between the constituent dU and dT single-stranded oligonucleotides (data not shown). Contaminating slower or faster bands were not observed.

The UV absorption spectra of ps-U1·U2 and aps-U1·U3 in the standard buffer systems exhibited the same characteristic features and ps/aps distinctions (Figure 2A1 and A2) previously described for the corresponding duplexes consisting of d(A·T) base pairs (ps-D1·D2 and aps-D1·D3). The low-temperature (ps helix − aps helix) difference spectra were very similar (Figure 2C1 and C2), with a maximum near 255 nm, a minimum near 283 nm, and an isosbestic point near 265 nm.

Helix–Coil Transitions

The thermal transitions of the various duplexes were measured by uv absorption and are depicted in Figure 3 and summarized in Table I. The ps-U1·U2 duplex exhibited a hyperchromicity profile (Figure 3B) very similar to that measured previously for ps-D1·D2,[2,5] albeit with a slightly lower magnitude and with a more distinct peak in the 260–265 region. The spectral manifestations accompanying the melting of aps-U1·U3 and aps-D1·D3[2,5] were also very similar both in shape and extent.

The thermodynamic comparisons between the ps and aps duplexes with different T/U substitutions are best appreciated by reference to Figure 4. In all cases, the aps species were more stable than their corresponding ps counterparts, in terms of T_m by 14° and in ΔG (at 25°C) by 18 kJ mol^{-1} (for all U-substituted molecules) and 32 kJ mol^{-1} for the reference T-containing molecules. The T_m decreased approximately linearly with the extent of T/U substitution for both the ps and aps species; the slope was ~ −0.5° per substitution. The sequence of transition enthalpy and entropies, however, differed between the ps and aps duplexes. In the latter case, all substituted molecules had approximately the same ΔH (~ 400 kJ mol^{-1}), dramatically less than the 620 kJ mol^{-1} for the parent aps-D1·D3 (Figure 4B). The transition entropy showed the same relative behavior. In contrast, the effect of T/U substitutions on the ps species was more complex (Figure 4A). T/U substitution in the mixed sequence segment of the molecule had the greatest effect on the reduction of ΔH and $T\Delta S$ (ps-D1·D2 → ps-D1·U2), but both parameters tended back toward the original values upon further substitution.

These results can be compared with the effects of T/U substitutions on simple sequence polymeric aps-DNA. In terms of T_m depression, the effect of 100% substitution is much greater on the homopolymer duplexes (dA·dT → dA·dU) than on the alternating copolymers (dAT → dAU)[2,5]; in 0.1 *M* NaCl, the ΔT_m is −13 and −3°C, respectively.[26]

Like ps-D1·D2,[8] ps-U1·U2 was strongly stabilized by Na^+ and Mg^{2+} ions. The T_m of ps-U1·U2 increased by about 15°C in the range of 0.1–0.5 *M* NaCl. Mg^{2+} was more effective in stabilizing both the ps and aps duplexes (Figure 5B); further addition of Na^+ had little effect (Figure 5A).

Strand Orientation from Pyrene Monomer–Excimer Fluorescence

The monomer–excimer fluorescence emission of duplexes 5′-labeled with pyrene can be used to assess strand orientation[6,12] (K. Rippe and T. M. Jovin, in preparation). This method was applied to the duplexes formed from the U-containing oligomers (Figure 6). As in the case of ps-D1·D2, pyrene-labeled ps-U1·D2 exhibited the broad emission band around 490 nm characteristic of the excimer and thus indicative of a ps orientation of the two strands.[6,12] However, for ps-D1·U2 and ps-U1·U2 the excimer emission was strongly reduced (Figure 6).

A comparison of the fluorescence emission spectra of the pyrene-labeled single-stranded oligonucleotides provided a rationale for these

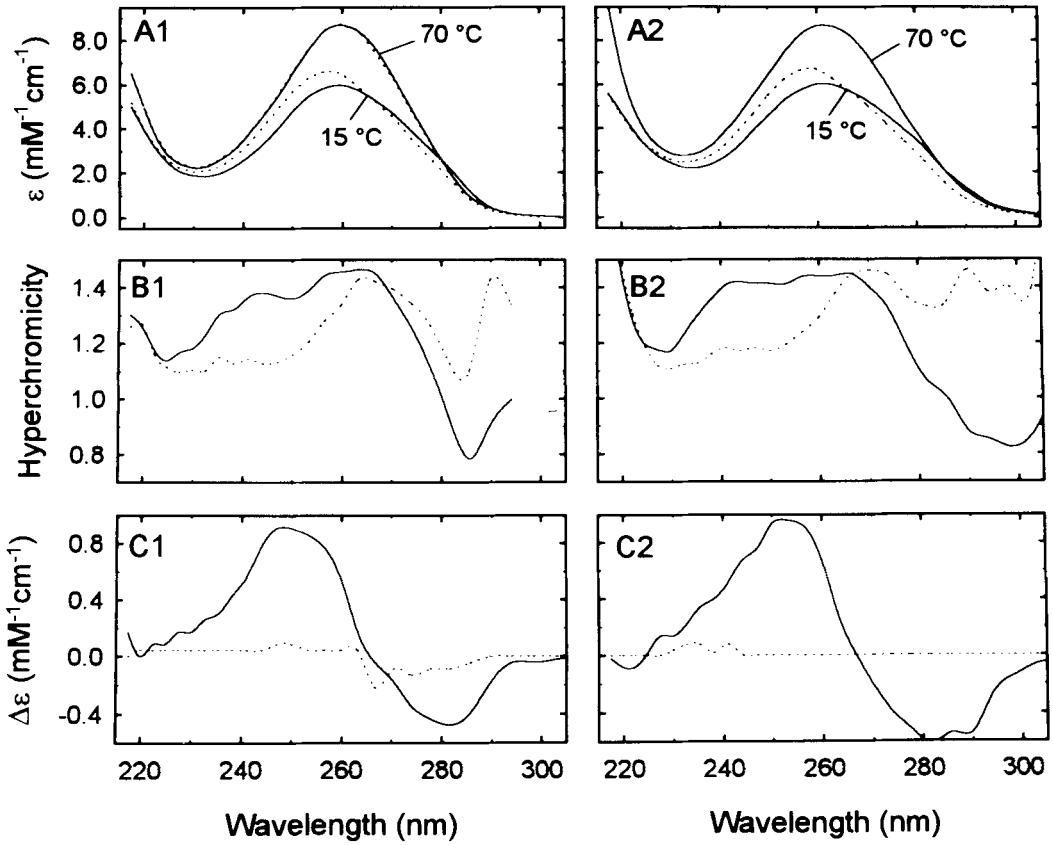

FIGURE 2 Spectroscopic properties of ps- and aps-DNA duplexes with d(A·U) base pairs (A1, B1, C1) and with d(A·T) base pairs (A2, B2, C2). (A1, A2). The uv spectra at 15 and 70°C; ps-U1·U2 (A1, ----) and aps-U1·U3 (A1, ——); ps-D1·D2 (A2, ----) and aps-D1·D3 (A2, ——). (B1, B2) Hyperchromicity spectra expressed as ratio of the absorbances at 70 and 15°C: ps-U1·U2 (B1, ----), aps-U1·U3 (B1, ——); ps-D1·D2 (B2, ----), aps-D1·D3 (B2, ——), (C1, C2) The uv difference spectra (C1, ps-U1·U2—aps-U1·U3; C2, ps-D1·D2—aps-D1·D3) at 15°C (——) and at 70°C (----).

differences. Although the characteristic structured emission spectra of the pyrene monomer at < 420 nm was observed in all cases (Figure 6, insert), the relative intensities varied greatly: D1 ≈ U1 ≫ U2 ≫ D2. As in previous studies, formation of the ps-duplex structures by addition of the complementary strand led to a marked reduction of the monomer emission and a corresponding emergence of the excimer emission centered at 490 nm (Figure 6). In the case of duplexes formed from the various combinations of the T- and U-containing pyrene-labeled strands, two classes were evident: D1·D2 = U1·D2 and U1·U2 = D1·U2. The first set of molecules exhibited the greater degree of monomer quenching and excimer formation. One can infer from these results that (a) the emission of pyrene coupled to the 5′-ends of homopyrimidine sequences (Figure 1) is greatly quenched relative to that of the complementary homopurine sequences, and (b) monomer quenching and excimer formation in duplex molecules is favored in duplexes with the 5′-T relative to the 5′-U strands. Thus, it appears that in the ps duplex molecules at least one of the pyrene partners interacts strongly (by stacking?) and preferentially with *trans* d(A·U) compared to *trans* d(A·T) base pairs. It has been proposed that the quenching of aromatic fluorophores by the bases of nucleic acids is due to a mechanism of photoinduced electron transfer; T and U differ in both oxidation and reduction potentials.[27] As expected, the T/U substitution in the 5′-purine strand had little or no effect on the fluorescence properties of the ps-DNAs. Thus, the ps orientation was established by this technique in all cases, in agreement with the postulated structures (Figure 1) and other experimental results presented below.

CD Spectroscopy

The analysis by CD spectroscopy of the ps and aps duplexes is shown in Figure 7. Ps-U1·U2 and aps-U1·U3 exhibited slight differences in the CD spectral range 260–290 nm in comparison with the corresponding ps-D1·D2 and aps-D1·D3 duplexes. In particular, the shoulder near 260 nm in the case of the T-containing ps duplex (curve 4) appeared as a maximum for the U-containing ps-DNA (curve 2). The latter also exhibited a depression near 285 nm in contrast to the peak of the aps-duplex (curve 1). The magnitude of the negative CD band around 248 nm was lower for both U-containing structures (curves 1 and 2).

The above CD features may be indicative of slight variations in the ps-duplex conformations due to the presence of *trans* d(A·U) instead of d(A·T) base pairs. In comparing the spectra of the 25-nt duplexes with those of poly(dA)·poly(dT) and poly(dA)·poly(dU),[28–31] we note the common negative band around 248 nm. There were, however, differences in the long wavelength region between 260 and 290 nm. Poly(dA)·poly(dT) shows a negative peak above 265 nm,[30,31] whereas poly(dA)·poly(dU) has positive CD signals at > 260 nm.[29,31] In the case of aps-D1·D3 and ps-D1·D2, a shoulder occurred near 260 nm with zero or negative values (Figure 7A, curves 3 and 4) in contrast to the clearcut positive dichroism at this wavelength of poly(dA)·poly(dT).[29–31] The positive peak at 285 nm of poly(dA)·poly(dU)[29,30] appeared in the spectrum of aps-U1·U3 (curve 1) but was absent in the spectrum of ps-U1·U2 (curve 2).

IR Spectroscopy

The equimolar mixture of U1 and U3 forms the double-stranded helix aps-U1·U3. In the ir spectra, this structure exhibited bands at 1697 and 1663 cm^{-1}, which are assigned to the C2=O2 and C4=O4 carbonyl stretching vibrations, respectively (Figure 8). The corresponding bands of the components oligonucleotides U1 and U3 were at lower frequencies, 1691 and 1660 cm^{-1}, respectively (Table II). The bands at 1624–1626 cm^{-1} of the individual strands were also shifted, appearing at 1629 cm^{-1} for the aps-U1·U3 duplex.

In contrast, the ir spectra at 5°C of an equimolar mixture of U1 and U2 (Figure 8), forming ps-U1·U2, were different from that of the aps-U1·U3. The reverse Watson–Crick base pairing in the parallel-stranded duplex[6,7] should displace both the C2=O2 and the C4=O4 carbonyl

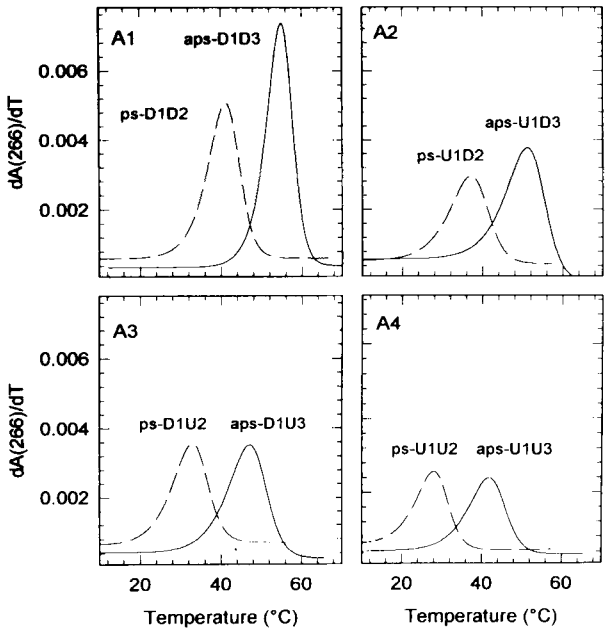

FIGURE 3A

FIGURE 3 Helix–coil transitions of duplexes with various combinations of T and U bases. (A) First derivative thermal profiles. (B) Thermally resolved uv absorption spectra of ps-U1·U2 and aps-U1·U3 helices. The ratio of $A(T)/A(T_0)$ is plotted vs temperature; T_0, initial temperature. Spectra were recorded in 10 m*M* $MgCl_2$, 10 m*M* Na-cacodylate, pH 7.

stretching vibrations from the positions adopted with the antiparallel duplex U1·U3, in which base pairing is conventional Watson–Crick. The C4=O4 and C2=O2 vibrations reflect hydrogen bonding in aps- and ps-DNA, respectively. Substitution of dT by dU should not change this distinction, but the bands might be expected to shift in position due to the different masses and force constants. The expected displacement of the C4=O4 carbonyl stretching vibration from 1665 cm^{-1} to higher wavenumbers was not observed. However, in the region of the C2=O2 carbonyl stretching vibration, the spectra of aps-U1·U3 and ps-U1·U2 differed significantly; the bands shifted from 1699 to 1692 cm^{-1}. We conclude that the ir spectra support the assumption of a formation of ps-U1·U2 at 5°C and under the experimental conditions. However, the spectral signature was less distinct than that observed previously for ps-D1·D2.[9] This circumstance may reflect the spectral perturbations induced by the T/U substitution but possibly the presence of an admixture of ps-DNA and mismatched aps-DNA as well.

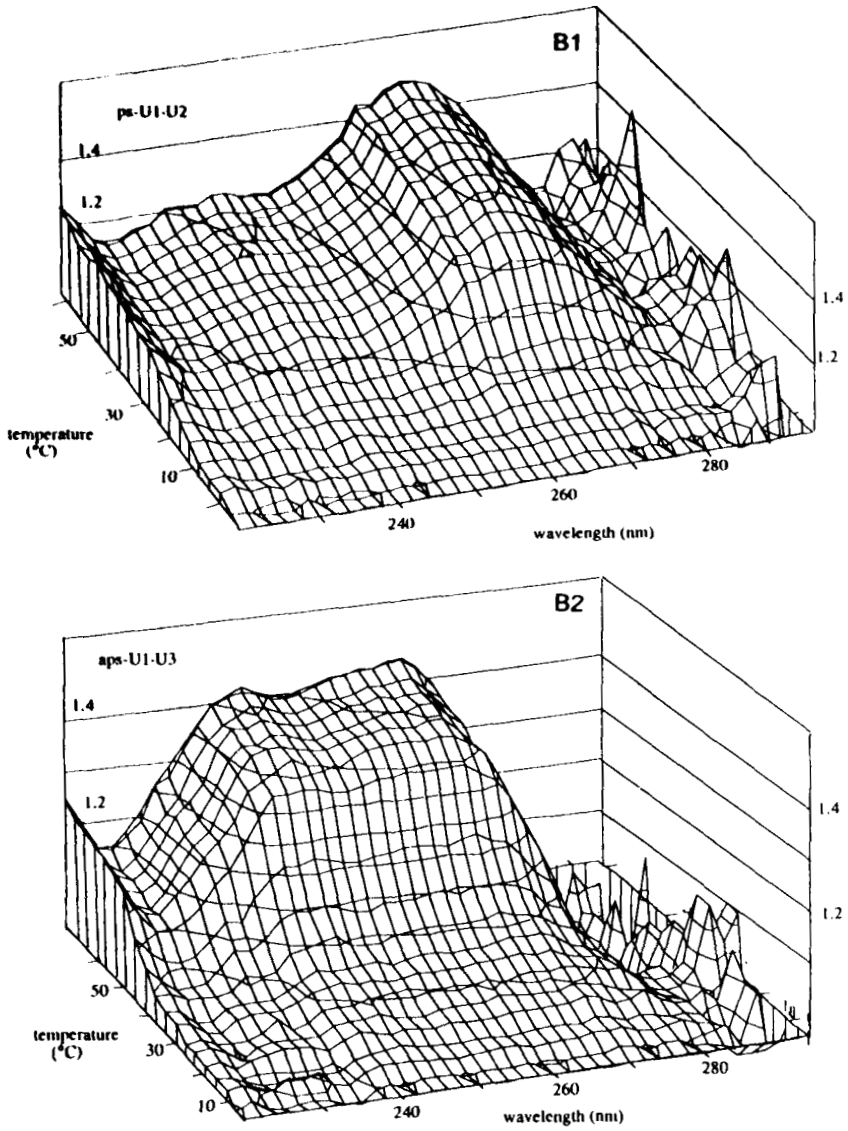

FIGURE 3B

The ir spectra of the hybrid duplexes ps-D1·U2 and ps-U1·D2 in D_2O at ~ 8°C also showed indications of base pairing. However, a minor fraction of ps-DNA was detected unambiguously only in the case of the duplex ps-U1·D2, for which spectral deconvolution indicated bands at 1684, 1668, and 1641 cm^{-1}. In contrast, these bands were not detected or were much weaker with ps-D1·U2, possibly reflecting the lower fractional T content of this hybrid species (Figures 1 and 4).

In summary, the substitution of dT by dU disfavors the formation of ps-DNA according to the ir spectral data, in accordance with the thermodynamic findings discussed above.

Drug Binding to ps-U1·U2

Binding studies of defined drugs to duplex DNA provide estimations of relative affinities for the ps- and aps-helices and are very useful for probing the underlying structural differences.[5] The affinity of the intercalating drug ethidium bromide for ps-DNA is higher than for aps-DNA, whereas the minor-groove specific dye Hoechst 33258 binds much less to the parallel-stranded helix.[5] Upon titration of an ethidium bromide solution with ps-U1·U2, the enhancement of fluorescence was significantly greater than for aps-U1·U3 (Figure 9A). The opposite effect was observed for Hoechst 33258 (Figure 9B). These differences in the binding prop-

Table I Parameters for the Helix–Coil Transitions of ps and aps Duplexes[a]

Duplex	T_m (°C)	$T_{m,corr}$ (°C)	ΔH_{vH} (kJ mol^{-1})	$T\Delta S$, 25°C (kJ mol^{-1})	ΔG, 25°C (kJ mol^{-1})
ps-D1·D2	40.3	39.9	466 (9)	406 (9)	60 (9)
ps-U1·D2	36.3	36.2	367	316	51
ps-D1·U2	31.9	31.6	393	347	46
ps-U1·U2	27.5	27.6	416 (17)	375 (16)	41 (16)
aps-D1·D3	54.2	53.8	620 (8)	528 (8)	92 (8)
aps-U1·D3	50.9	50.6	408	338	70
aps-D1·U3	46.3	46.1	399	335	64
aps-U1·U3	41.1	41.3	400 (12)	342 (12)	58 (11)

[a] The measurements were made in 10 m*M* Na-cacodylate, pH 7.0, 10 m*M* $MgCl_2$. The DNA strand concentrations varied in the range 0.97–1.35 μM, and the measured T_m values were corrected ($T_{m,corr}$) to a 1 μM reference concentration according to Ref. 17. Data analysis was according to Refs. 3 and 17, modified for derivative data. The values in parentheses are the relative magnitudes of the 95% confidence limits in percent derived from five experiments. In the case of hybrid duplexes, the number of measurements made do not suffice for a statistical evaluation. The sequences are given in Figure 1.

erties of the two dyes were in full agreement with the published data of the ps-D1·D2-helix[28] and indicative of the presence of the postulated ps conformation of the U1·U2 duplex.

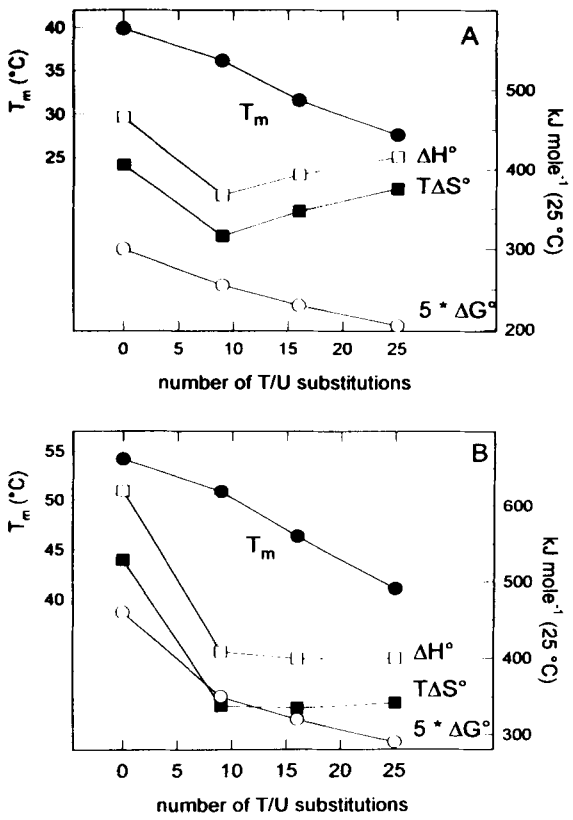

FIGURE 4 Dependence of thermodynamic parameters for the helix–coil transition on the number of T/U substitutions. (A) ps-DNA duplexes. (B) aps-DNA duplexes. Data from Table I.

Substrate Specificity for Nucleases

Nuclease activity on ps-DNA has been found to be generally lower than on conventional aps-DNA.[4,28] DNase I is specific for double-stranded B-DNA and induces single-strand breaks.[32] It is inactive on ps-DNA.[4,28] The susceptibilities of ps-U1·U2 and aps-U1·U3 to hydrolysis by DNase I was determined (Figure 10). Data for the corresponding ps-D1·D2 and aps-D1·D3 duplexes were also obtained for comparison (Figure 10, lanes 1,2 and 5,6). DNase I exhibited extremely low activity for both ps-D1·D2 (lane 5) and ps-U1·U2 duplex (lane 7). In contrast, both aps duplexes were completely degraded by the enzyme (lanes 6 and 8). Very similar

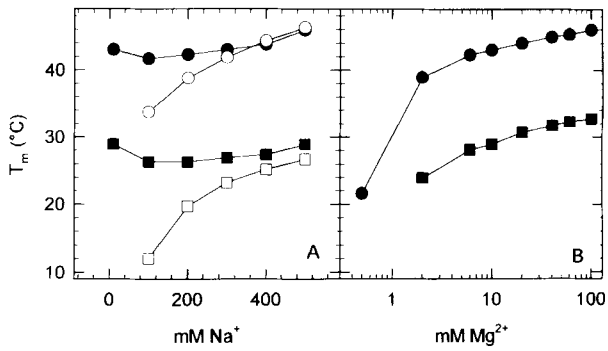

FIGURE 5 Melting temperature change of ps-U1·U2 (squares) and aps-U1·U3 (circles) as a function of increasing Na^+ and Mg^{2+} concentration. (A) Hollow symbols, increasing [Na^+] without Mg^{2+} in the buffer solution; solid symbols, increasing [Na^+] with 10 m*M* $MgCl_2$ in the buffer solution. (B) Increasing concentration of Mg^{2+} with 10 m*M* Na-cacodylate in the buffer solution.

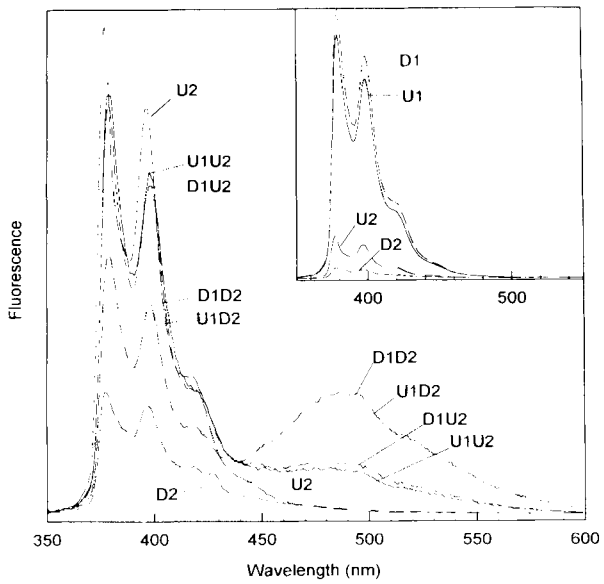

FIGURE 6 Fluorescence emission spectra of pyrene-labeled oligonucleotides and duplex structures. Measurements in 10 m*M* $MgCl_2$, 10 m*M* Na-cacodylate at 4°C; λ_{exc} = 340 nm. Inset: comparison of pyrene-labeled oligonucleotides D1,U1 and D2,U2.

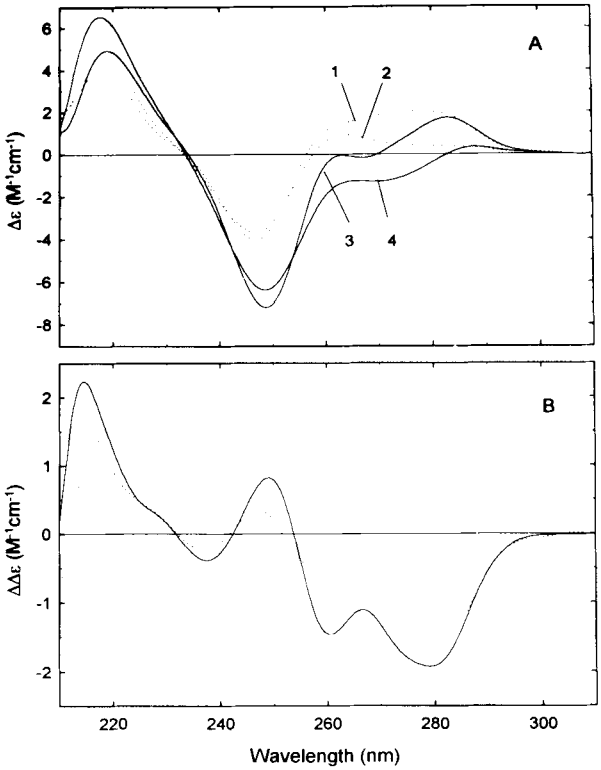

FIGURE 7 CD data of ps and aps duplexes. (A) CD spectra of aps-U1·U3 (1), ps-U1·U2 (2), aps-D1·D3 (3), and ps-D1·D2 (4). (B) CD difference spectra (ps–aps) of the d(A·U) duplex (----) and d(A·T) duplex (——).

behavior was found for exonuclease III (data not shown). According to previous interpretations,[4,28] the drastic lowering of the enzymatic cleavage rate with ps substrates is probably related to changes in the groove dimensions; ps-DNA lacks the minor groove and stereospecific interaction loci of B-DNA recognized by DNAse I.[33] The T/U substitution does not render ps-DNA more susceptible to the enzyme.

Model Structures

The conformations of the 25-mer ps and aps duplexes constructed from either the dT or dU containing oligonucleotides were constructed as described under Materials and Methods and are depicted in Figure 11 (see also Table III). The D1 and U2 strands were placed in approximately the same position in all the depicted structures to facilitate comparison. One can easily perceive the parallel orientation of the strands, the presence of reverse Watson–Crick base pairing, and the equivalent grooves of the ps-DNA models. The replacement of the C5 methyl group of T by the hydrogen atom in U leads to alterations in the surface topology of the nucleic acids. One significant feature is the restriction of the methyl (or H) groups to the major groove of the aps helices, compared to the se-

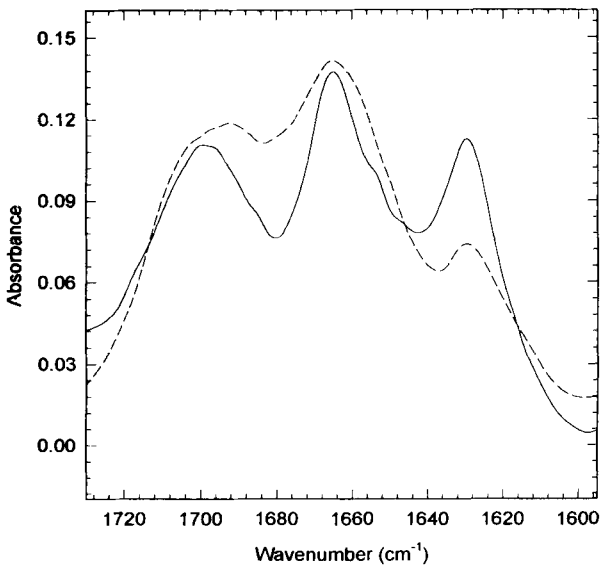

FIGURE 8 Infrared spectra of ps-U1·U2 (----) and aps-U1·U3 (——) in D_2O solution at 5°C. The spectra are displayed in the frequency region of 1595–1720 cm^{-1}. The abscissa is given in arbitrary absorbance units.

Table II IR Spectra (D_2O Solution)

		Wavenumbers of the Absorption Maxima (in cm^{-1})				
U1		1690		1659		1626
U2		1697	1685	1655		1623
U3		1692		1657		1624
ps-U1·U2	5°C	1691	1686	1664		1626
aps-U1·U3		1697		1663		1629
ps-U1·D2	ca. 8°C	1996	1685	1668	1641 1654	1624
ps-D1·U2	ca. 8°C	1693	(1685)	1664	1655	1626
ps-D1·D2			1685	1668	1641	1622
aps-D1·D3		1696		1663	1641	1622
$d(T)_{10}$		1692		1663		1632

quence-dependent distribution in both grooves of ps-DNA (Table III). In another study, it has been established that the net hydration of the ps-D1·D2 and aps-D1·D3 duplexes is very similar (V. Buckin and T. M. Jovin, submitted). One would surmise from the present investigation that the T/U substitution should affect the distribution of bound water differentially in the two conformations.

CONCLUSIONS

The evidence that d(A·U) base pairs can exist in stable parallel-stranded helices extends the knowledge about this alternative conformation of DNA. However, the thermodynamic and spectral data and the modeling calculations reveal significant differences induced by the replacement of dT by

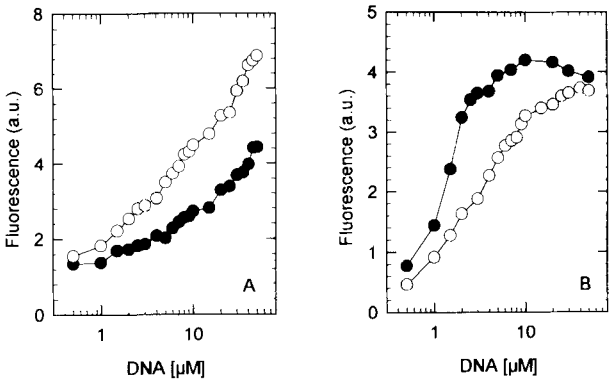

FIGURE 9 Drug binding experiments to ps-U1·U2 and aps-U1·U3 of ethidium bromide (A) and Hoechst 33258 (B) in 10 m*M* Na-cacodylate and 2 m*M* $MgCl_2$ at 4°C. Ethidium bromide: λ_{exc} = 520 nm, λ_{em} = 610 nm; Hoechst 33258: λ_{exc} = 355 nm, λ_{em} = 465 nm. Titration of the drugs (0.5 μM) with ps-U1·U2 (empty circles) and aps-U1·U3 (filled circles).

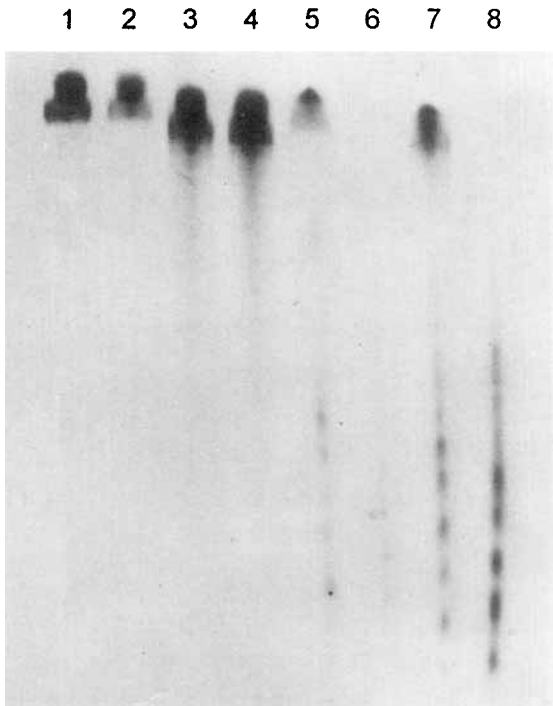

FIGURE 10 DNase I digest of ps- and aps-DNA duplexes. Incubation of 8 units enzyme per nmole nucleotide in Tris buffer (see Materials and Methods) at 4°C for 2 h. The reaction was stopped by addition of EDTA to 20 m*M* and heating to 60°C for 5 min. Eighty microliters of each sample were run in a denaturing gel. Without DNase I: lanes: (1) ps-D1·D2; (2) aps-D1·D3; (3) ps-U1·U2; (4) aps-U1·U3. DNase I digests: lanes: (5) ps-D1·D2; 6, aps-D1·D3; (7) ps-U1·U2; (8) aps-U1·U3.

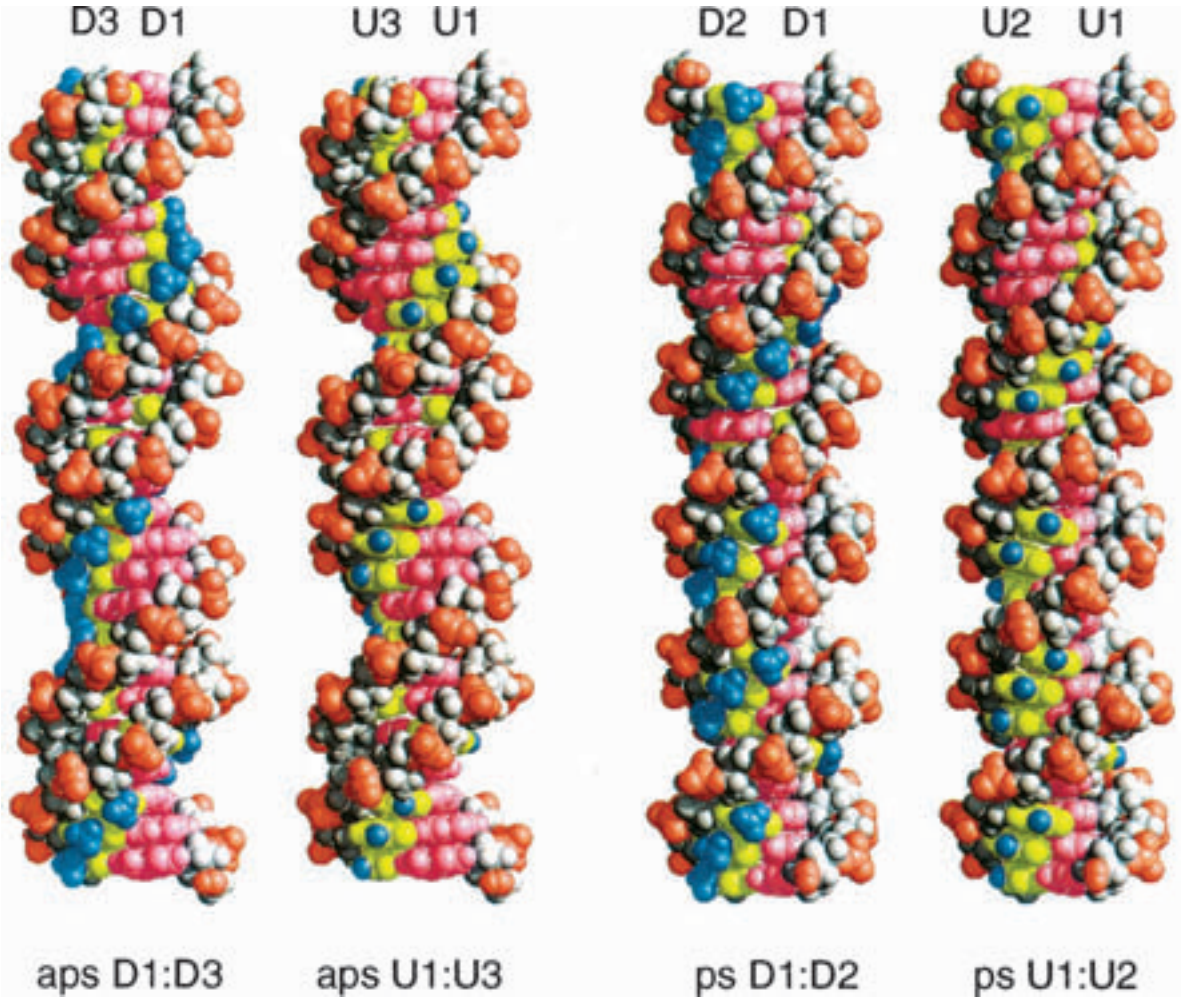

FIGURE 11 CPK models of the minimized aps-D1·D3, aps-U1·U3 and ps-D1·D2, ps-U1·U2 structures. The D1,U1 5′ end starts at the upper right end of the two DNA structures. Color coding of the DNA elements: gray, sugar backbone; red, phosphate groups including O3′ and O5′; magenta, adenine; yellow, thymine/uracil; blue, thymine methyl groups/uracil H5.

dU. Thus, while the decrease in T_m was related approximately linearly to the number of T/U substitutions (Figure 4), the more complete thermodynamic analysis revealed more subtle effects (Table III). The introduction of isolated d(G·C) base pairs[5] also destabilizes the parent 25-nt sequences analyzed in this report (Figure 1). From these results we conclude that the methyl group of the pyrimidine in a secondary structure based on reverse Watson–Crick base pairing plays a significant role in the stabilization of the ps double helix. Inasmuch as a stable ps-RNA has yet to be described, it also appears that in addition to the base the nature of the sugar moiety in the backbone is essential in determining the stability of potential ps duplex structures.

Table III Helical Parameters of the DNA Conformers

Duplex	Average Twist (°)	Average Rise (Å)
aps-D1·D3	40.6	3.2
aps-U1·U3	41.5	3.2
ps-D1·D2	41.2	3.2
ps-U1·U2	41.5	3.2

The location and reactivity of base-specific groups in the grooves of double-stranded DNA

provide the recognition elements for small ligands, such as nonintercalating drugs and proteins, and thus for distinguishing nucleotide sequence and associated secondary structure.[33,34] The effects of the rather conservative substitution of dT by dU in the defined set of ps and aps duplex structures selected for this investigation help define further the operative rules underlying the phenomenon of stereospecific recognition.

This work was supported by the Deutsche Forschungsgemeinschaft (grants Zi 396/2-1 and Jo 105/7-1). The authors wish to thank Dr. S. Winter, Institute of Molecular Biotechnology Jena, for assistance in the fluorescence measurements.

REFERENCES

1. Ramsing, N. B. & Jovin, T. M. (1988) *Nucleic Acids Res.* **16,** 6659–6676.
2. Rippe, K., Ramsing, N. B. & Jovin, T. M. (1989) *Biochemistry* **28,** 9536–9541.
3. Ramsing, N. B., Rippe, K. & Jovin, T. M. (1989) *Biochemistry* **28,** 9528–9535.
4. Rippe, K. & Jovin, T. M. (1989) *Biochemistry* **28,** 9542–9549.
5. Rippe, K., Ramsing, N. B., Klement, R. & Jovin, T. M. (1990) *J. Biomol. Struct. Dynam.* **7,** 1199–1209.
6. Rippe, K. & Jovin, T. M. (1992) *Methods Enzymol.* **211,** 199–220.
7. van de Sande, J. H., Ramsing, N. B., German, M. W., Elhorst, W., Kalisch, B. W., v. Kitzing, E., Pon, R. T., Clegg, R. M. & Jovin, T. M. (1988) *Science* **241,** 551–557.
8. Otto, C., Thomas, G. A., Rippe, K., Jovin, T. M. & Peticolas, W. L. (1991) *Biochemistry* **30,** 3062–3069.
9. Fritzsche, H., Akhebat, A., Taillandier, E., Rippe, K. & Jovin, T. M. (1993) *Nucleic Acids Res.* **21,** 5085–5091.
10. Pattabiraman, N. (1986) *Biopolymers* **25,** 1603–1606.
11. Kuryavyi, V. V. (1987) *Molek. Biol.* (Russ.) **21,** 1486–1496.
12. Rippe, K., Fritsch, V., Westhof, E. & Jovin, T. M. (1992) *EMBO J.* **11,** 3777–3786.
13. Rentzeperis, D., Rippe, K., Jovin, T. M. & Marky, L. A. (1992) *J. Am. Chem. Soc.* **114,** 5926–5928.
14. Tchurikov, N. A., Shchyolkina, A. K., Borissova, O. F. & Chernov, B. K. (1992) *FEBS Lett.* **297,** 233–236.
15. Shchyolkina, A. K., Borissova, O. F., Chernov, B. K. & Tchurikov, N. A. (1994) *J. Biomol. Struct. Dynam.* **11,** 1237–1249.
16. Garcia, A. E., Soumpasis, D. M. & Jovin, T. M. (1994) *Biophys. J.* **66,** 1742–1755.
17. Evertsz, E. M., Rippe, K. & Jovin, T. M. (1994) *Nucleic Acids Res.* **22,** 3293–3303.
18. Robinson, H., van Boom, J. H. & Wang, A. H.-J. (1994) *J. Am. Chem. Soc.* **116,** 1565–1566.
19. Liu, K., Miles, H. T., Frazier, J. & Sasisekharan, V. (1993) *Biochemistry* **32,** 11802–11809.
20. Kang, C. H., Berger, I., Lockshin, C., Ratliff, R., Moyzis, R. & Rich, A. (1994) *Proc. Natl. Acad. Sci. USA* **91,** 11636–11640.
21. Gehring, K., Leroy, J.-L. & Guéron, M. (1993) *Nature* **363,** 561–565.
22. Pearlman, D. A., Case, D. A., Caldwell, J. C., Seibel, G. L., Singh, U. C., Weiner, P. & Kollman, P. A. (1991) AMBER 4.0, University of California, San Francisco.
23. Connoly, M. L. (1983) *Science* **221,** 709–713.
24. Soumpasis, D. M. & Tung, C. S. (1988) *J. Biomol. Struct. Dynam.* **6,** 397–420.
25. Zmudzka, B., Bollum, F. J. & Shugar, D. (1969) *J. Mol. Biol.* **46,** 169–183.
26. Fasman, G. D., Ed. (1975) *Handbook of Biochemistry and Molecular Biology, 3rd Ed., Nucleic Acids—Vol. I,* CRC Press, Cleveland, OH, p. 575.
27. Dapprich, J. (1994) Ph.D. thesis, Georg-August University, Göttingen, Germany.
28. Jovin, T. M., Rippe, K., Ramsing, N. B., Klement, R., Elhorst, W. & Vojtišková, M. (1990) in *Structure & Methods, Vol. 3: DNA & RNA,* Sarma, R. H. & Sarma, M. H., Eds., Adenine Press, Schenectady, NY, pp. 155–174.
29. Zimmer, Ch., Kakiuchi, N. & Guschlbauer, W. (1982) *Nucleic Acids Res.* **10,** 1721–1732.
30. Steely, H. T., Gray, D. M. & Ratliff, R. L. (1986) *Nucleic Acids Res.* **24,** 10071–10090.
31. Gray, D. M., Ratliff, R. L. & Vaughan, M. R. (1992) *Methods Enzymol.* **211,** 389–406.
32. Campbell, V. W. & Jackson, D. A. (1979) *J. Biol. Chem.* **255,** 3726–3735.
33. Sucle, D., Lahm, A. & Oefer, C. (1988) *Nature* **332,** 464–468.
34. Seeman, N. C., Rosenberg, J. M. & Rich, A. (1976) *Proc. Natl. Acad. Sci. USA* **73,** 804–808.